

# Visual Navigation Support for Liver Applicator Placement using Interactive Map Displays

J. Hettig<sup>1</sup>, G. Mistelbauer<sup>2</sup>, C. Rieder<sup>3</sup>, K. Lawonn<sup>4</sup> and C. Hansen<sup>1</sup>

<sup>1</sup>Computer-Assisted Surgery Group, Faculty of Computer Science, University of Magdeburg, Germany

<sup>2</sup>Visualization Group, Faculty of Computer Science, University of Magdeburg, Germany

<sup>3</sup>Fraunhofer MEVIS, Bremen, Germany

<sup>4</sup>Institute for Computational Visualistics, University of Koblenz-Landau, Germany

The definite version of this article is available at <http://diglib.eg.org/>

## **To cite this version:**

Hettig, J., Mistelbauer, G., Rieder, C., Lawonn, K., Hansen C.

Visual Navigation Support for Liver Applicator Placement using Interactive Map Displays

Proc. of Eurographics Workshop on Visual Computing for Biology and Medicine (EG VCBM), in print, 2017

# Visual Navigation Support for Liver Applicator Placement using Interactive Map Displays

J. Hettig<sup>1</sup>, G. Mistelbauer<sup>2</sup>, C. Rieder<sup>3</sup>, K. Lawonn<sup>4</sup> and C. Hansen<sup>1</sup>

<sup>1</sup>Computer-Assisted Surgery Group, Faculty of Computer Science, University of Magdeburg, Germany

<sup>2</sup>Visualization Group, Faculty of Computer Science, University of Magdeburg, Germany

<sup>3</sup>Fraunhofer MEVIS, Bremen, Germany

<sup>4</sup>Institute for Computational Visualistics, University of Koblenz-Landau, Germany

---

## Abstract

*Navigated placement of an ablation applicator in liver surgery would benefit from an effective intraoperative visualization of delicate 3D anatomical structures. In this paper, we propose an approach that facilitates surgery with an interactive as well as an animated map display to support navigated applicator placement in the liver. By reducing the visual complexity of 3D anatomical structures, we provide only the most important information on and around a planned applicator path. By employing different illustrative visualization techniques, the applicator path and its surrounding critical structures, such as blood vessels, are clearly conveyed in an unobstructed way. To retain contextual information around the applicator path and its tip, we desaturate these structures with increasing distance. To alleviate time-consuming and tedious interaction during surgery, our visualization is controlled solely by the position and orientation of a tracked applicator. This enables a direct interaction with the map display without interruption of the intervention. Based on our requirement analysis, we conducted a pilot study with eleven participants and an interactive user study with six domain experts to assess the task completion time, error rate, visual parameters and the usefulness of the animation. The outcome of our pilot study shows that our map display facilitates significantly faster decision making (11.8 s vs. 40.9 s) and significantly fewer false assessments of structures at risk (7.4 % vs. 10.3 %) compared to a currently employed 3D visualization. Furthermore, the animation supports timely perception of the course and depth of upcoming blood vessels, and helps to detect possible areas at risk along the path in advance. Hence, the obtained results demonstrate that our proposed interactive map displays exhibit potential to improve the outcome of navigated liver interventions.*

## CCS Concepts

•**Human-centered computing** → **Scientific visualization**; **Pointing devices**; •**Computing methodologies** → **Non-photorealistic rendering**; •**Applied computing** → **Health informatics**;

---

## 1. Introduction

Medical navigation systems within an operating room proved to be able to efficiently support applicator guidance, e.g., for microwave ablation of lesions, during liver surgery [BBW\*14, SPY\*15, BMT\*16]. An important component of such a navigation system is the navigation screen that visualizes 3D anatomical structures (preoperative planning models) of interest together with the tracked surgical instruments. For liver surgery, these 3D structures contain the liver surface, lesions, and the liver vasculature. As shown in Fig. 1a, the common setting within an operating room provides only a small display for the surgeons, without enough space for complex visualization or interaction. Consequently, the representation of the anatomical structures has to change depending on the procedure step, e.g., between a visualization of 3D anatomical structures (Fig. 1a) and a multiplanar reformation (MPR) (see Fig. 1b) of the underlying radiological image data. While the 3D visualization provides a good overview, interesting structures might be obstructed. The radiolog-

ical images show more detail, but adjacent information is lacking. Furthermore, tumors and vasculature look alike without contrast agent or the used windowing is inferior. In both cases it might be necessary to delegate complex interaction tasks to an assistant, or interrupt the intervention and set instruments aside to navigate through the data.

Our approach aims to strip the superfluous information from the preoperative models, reduce the unnecessary interaction and provide only the information required during the applicator placement. We propose a method to generate an interactive as well as an animated (predictive) map display using cutaway surfaces and illustrative contour rendering. This enables a simple and fast assessment of risk structures without the need to interact with the visualization. To evaluate our visualization concept, we conducted a static pilot study with eleven participants by comparing our approach with a conventional 3D visualization (that is used for liver navigation systems) regarding task completion time and error rate. A second interactive user study

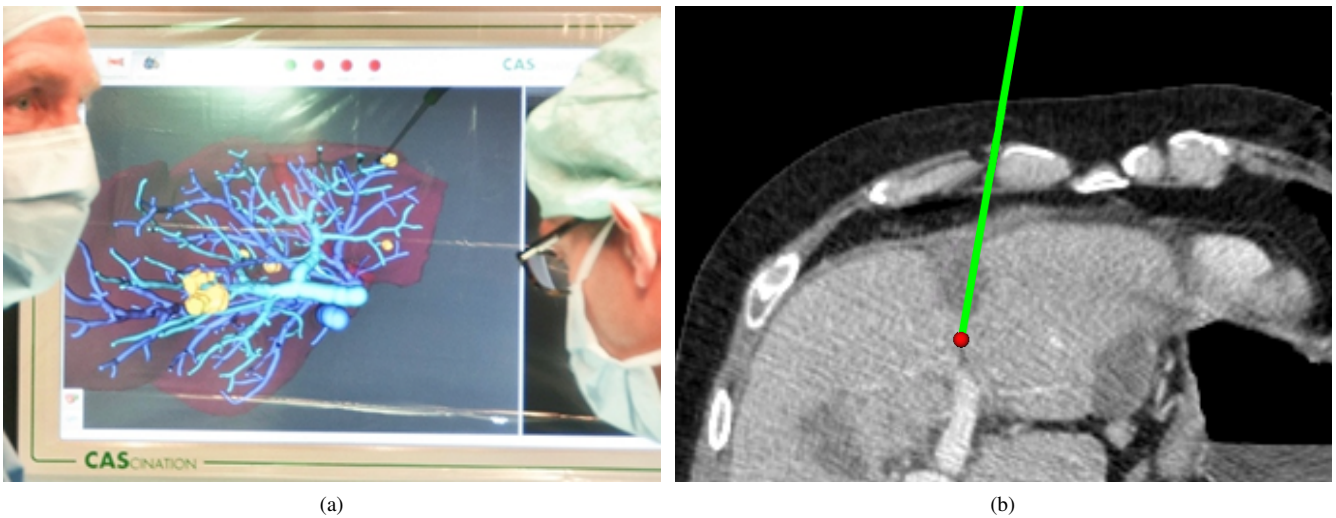


**Figure 1:** Common setup of an operating room for applicator pathway navigation during liver surgery. (a) Visualization of 3D anatomical structures of the liver in the operating room using a surgical navigation system (CASINATION AG, Bern) and (b) an MPR of a CT data set with a tracked applicator (green) of a navigation system. Image courtesy of University Hospital Mainz, Germany.

was conducted with domain experts, to evaluate the visual appearance of the displays and the added value by means of predictive animation. The contributions of this paper are the following:

- We created a map display aiding navigated applicator placement along a specific path within the liver.
- We provide an algorithm to calculate the parts of the map display. Therefore, standard clipping planes are extended with a texture-based technique to visualize the cutaway surface. Illustrative contour lines are utilized as context information.
- We present a new method, predictive echo animation (PEA), using animation to visualize (predict) upcoming anatomical structures on the planned path.
- We evaluated our approach in a quantitative pilot and interactive user study.

## 2. Related Work

Most visualization methods for liver surgery are designed for pre-operative exploration of relevant critical anatomical structures such as tumors or blood vessels, as comprehensively overviewed by Schenk et al. [SHP11]. However, preoperative planning approaches are not directly transferable to the operating room. As it is important that surgeons focus on the operating field during an intervention, their interaction possibilities as well as field of view are limited. Therefore, the presentation of additional important information during surgery should follow the focus & context paradigm, i.e., highlighting relevant or critical structures while retaining contextual information of surrounding anatomical structures in an illustrative fashion [VKG04, SCC\*04]. Navigating within the data should be intuitive and simple to avoid cumbersome and time-consuming interactions in order to reveal relevant anatomical structures. During liver surgery, the attention should be focused on the structures that are located in close proximity to the instrument's tip. However, ef-

fective visualization methods that support interventions are rare. Subsequently, we describe the most common approaches.

Lamata et al. [LJPLD08] propose a visualization technique for liver resection surfaces in two different views. While a coronal view shows the resection surface, liver surface, nearby blood vessels, and tumors from the surgical perspective, a sagittal view presents these anatomical structures perpendicular to the surgeon's viewing direction. Informal assessments gathered in a user study indicate that the provided visualization increases the surgeon's confidence and sense of spatial orientation [LLS\*10]. An extension to this concept using an algorithm for surgical risk analysis was proposed by Hansen et al. [HZS\*10]. They propose methods for the identification and classification of critical anatomical structures in the vicinity of a preoperatively planned resection surface. Shadow-like distance indicators are introduced to visually encode the distance from the resection surface to these critical structures on a map. The approach was evaluated in a user study with ten surgeons [HZR\*13]. Therein, the method was integrated in a surgical navigation system and static scenes of the risk map together with a surgical instrument were presented. According to the results of their study, surgeons are significantly faster, make fewer errors, and interact less with the software application when using a map. However, the approaches Lamata et al. and Hansen et al. represent are not adapted to the non-interactive intraoperative situation and their value for applicator placement might be limited.

Several map displays to support surgical planning have been proposed. Navkar et al. [NTS\*10] and Herghelegiu et al. [HMP\*12] describe access maps for neurosurgery to assist surgeons in selecting an access path to a target tumor location while avoiding delicate or critical structures, such as blood vessels. For this reason, the blood vessels are projected on the skin model of the patient's head. The distance of these vessels to the skull or safe entry regions are color-coded, respectively. A preliminary evaluation study indicates

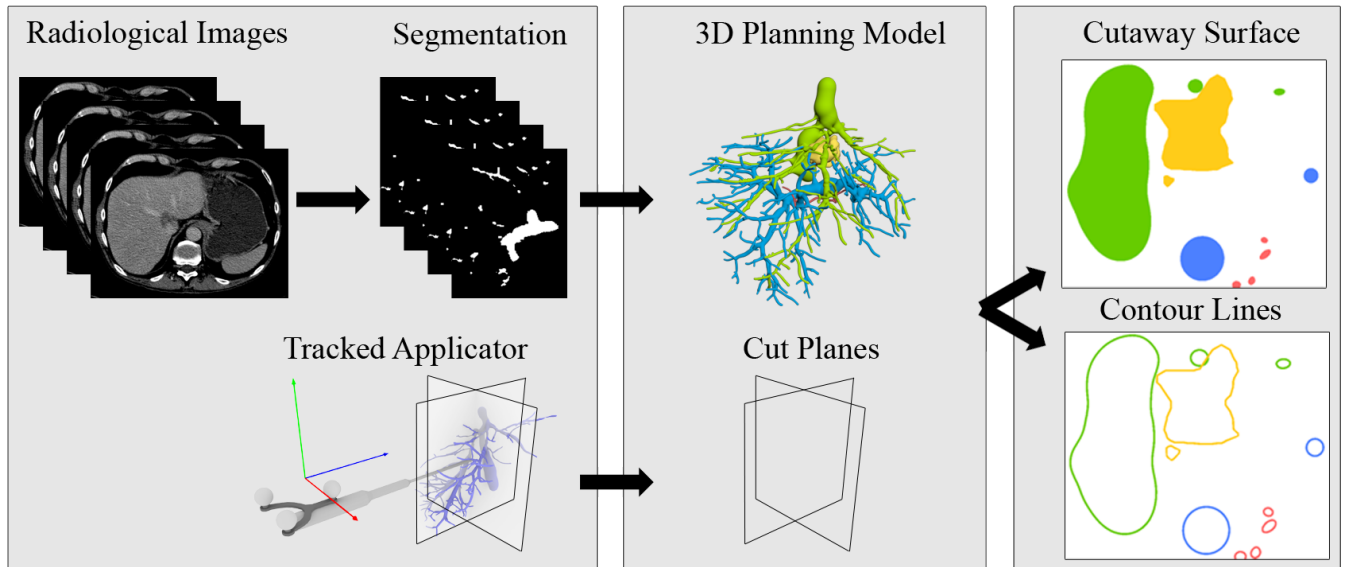


**Figure 2:** Input data and visualization pipeline of our map display. Radiological images serve as an input that are segmented for the generation of 3D planning models. Two planes positioned and orientated on a tracked applicator tip based on the local coordinate system define the cut planes. Planning models and planes are used for the calculation of cutaway surface and contour lines and allow the composition of various 2D map display.

that these maps provide efficient planning support for procedures such as biopsy, tumor ablation, and deep brain stimulation.

In the field of radiofrequency ablation planning, Rieder et al. [RWS\*10] introduced a visualization technique they refer to as *tumor map*. It depicts a pseudo-cylindrical mapping of a color-coded 3D tumor surface onto a 2D map. Colors encode simulated post-interventional coagulation zones. The tumor map allows for immediate detection of residual tumor tissue, and thus provides an effective way to assess the treatment outcome. A related approach for cerebral aneurysm surfaces is presented by Neugebauer et al. [NGB\*09]. They map the wall shear stress of a 3D blood flow simulation onto a 2D map. This provides an overview visualization on the map and a bidirectional link to the 3D data. As the approaches of Rieder et al. and Neugebauer et al. are designed to support preoperative planning and postoperative assessment, their value during an interventions remains unclear.

Cutaway or peeling illustrations are widely-used for medical and non-medical visualization, e.g., anatomy books [NC\*89] and construction plans, to focus on initially obstructed relevant structures. Burns and Finkelstein [BF08] introduced the generation of cutaway renderings for polygonal models. This technique allows exposure of objects of interest in the surrounding context. Liang et al. [LCKM05] present a method to cutaway predefined shapes of a polygonal model for orthopedic surgery. This obtains the shape of the surrounding structures and gives insight to hidden objects. Viola et al. [VKG04] presented an importance-driven visualization for volume renderings with an automatic focus and context display, utilizing a generalization of cutaway views. Thus, more important structures are displayed fully, and other unimportant structures more sparsely to prevent occlusion. Bruckner et al. [BGKG05] introduced visualization methods

for context-preserving illustrations using a feature-driven approach with different transparent transfer functions and clipping methods. Their approach represents an alternative to conventional techniques, including an easy and intuitive user control, but does not suffer from missing context information. Birkeland et al. [BBBV12] use an elastic membran for clipping volume data to preserve specific features of interest. Díaz et al. [DMNV12] make use of editing techniques based on clipping planes, extrusion and illustrative methods to interactively generate context-preserving visualizations of volume data.

A comprehensive mathematical survey of feature lines techniques was presented by Lawonn and Preim [LP16]. For illustrative rendering techniques for liver surgery, Hansen et al. [HWR\*10] presented a visualization method for augmented reality. They used distance-encoded silhouettes and surfaces to reduce the visual complexity of 3D planning models. Another approach for liver surgery was presented by Lawonn et al. [LLPH15]. They used an illustrative rendering technique to support depth perception on static images using a combination of supporting lines, view-aligned quads, and illustrative shadows. Moreover, hatching with different line styles is utilized to encode distances.

### 3. Material and Methods

For safe and confident placement of an applicator, surgeons require information about critical anatomical structures that are located either around a planned path or in front of the applicator's tip. In this section, we start with the definition of criteria for our visualization in a requirement analysis. This is followed by a description of the input data and the visualization algorithms of our proposed interactive map display (see Fig. 2). Subsequently, we explain an extension of

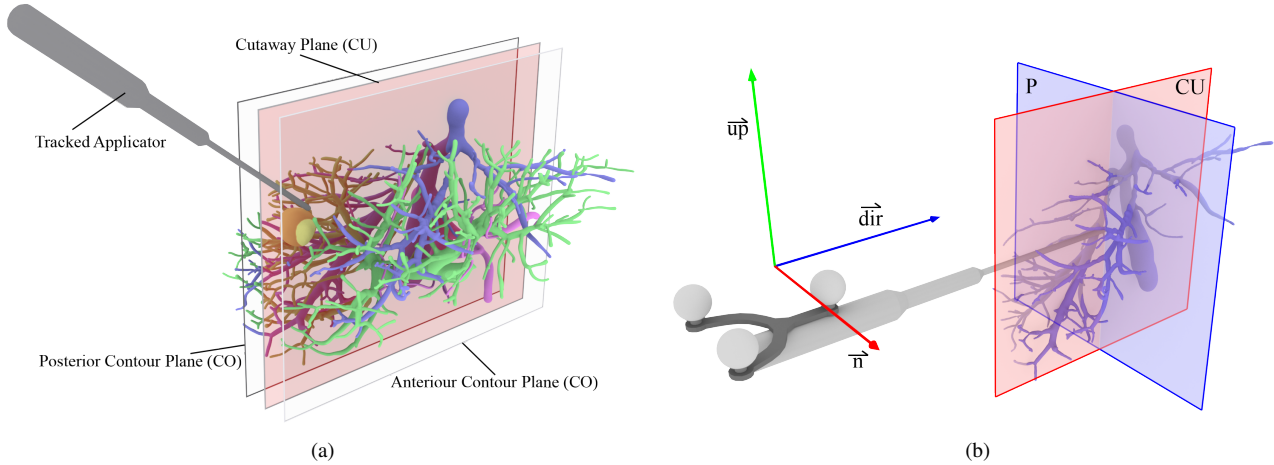


**Figure 3:** (a) Overview of the 3D models with a tracked instrument. The transparent planes show the position and orientation of cutaway surface and contour lines. (b) Tracked ablation applicator with local coordinate system. Vectors are as follows:  $\vec{n}$  red,  $\vec{up}$  green and  $\vec{dir}$  blue. Fixed on the applicator's tip are the planes CU (blue) and P (red).

the simple map display and present our predictive echo animation in detail. Furthermore, we demonstrate some examples of different cases and show the advantages of our visualization. Finally, we briefly explain how to visually link two map display visualizations.

### 3.1. Requirement Analysis

To support the placement of an applicator, an effective intra-operative visualization should reduce the visual complexity and only display the most important information on and around a planned path. Additionally, the interaction with the visualization should not distract the surgeon or interrupt their workflow. Those criteria are based on our observations and interviews with domain experts. Accordingly, the following requirements have to be met:

- The interaction with the visualization should depend on the position and orientation of the tracked applicator. No additional interaction should be necessary.
- The visualization should display all relevant information (e.g. critical structures such as blood vessels) along the path. This should facilitate surgeons a fast and error-free assessment of anatomical structures, compared to conventional 3D visualizations.
- The PEA should provide a quick overview about upcoming anatomical structures and a visual encoding of depth as well as distance information.

### 3.2. Input Data

Our approach is based on preoperatively acquired CT and MRI images from the patient's liver. These images are segmented by domain experts to extract the vasculature (portal vein, hepatic vein and hepatic artery), lesions (tumors and cysts), and the liver. Based on this segmentation result, 3D geometric models are generated using the medical image processing platform MeVisLab [RBH\*11]. These 3D models associated with the information of the tracked applicator are then further used to generate a cutaway surface and contour lines for our interactive map display (see Fig. 2).

### 3.3. Map Display

To offer surgeons a concise and expressive overview map for live application navigation, we provide several different map displays of the information around (out-of-plane) and along (in-plane) the applicator's path. The latter part of the map display is established using cutaway (surface) visualization, whereas the former employs illustrative contour rendering for the contextual information (see Fig. 2 right). An additional view in front of the applicator shows surrounding information in the direction of the path, which is then extended using an echo sounding approach (PEA) and is linked with the other views. This linked setup provides surgeons with only the necessary information in close proximity around the applicator and does not distract them with unnecessary complicated interaction to reveal this information.

**Interaction using a Tracked Instrument.** Our visualization is solely controlled by an tracked ablation applicator. To achieve this, the local coordinate system of the instrument is used to define two primary planes *CU* and *P* that are centered in the applicator's tip (see Fig. 3b). The first primary cutaway plane *CU* is spanned using the instrument's up vector  $\vec{up}$  and direction vector  $\vec{dir}$ . Two additional contour planes *CO* have a positive and negative offset  $\delta$  in the direction of this plane's normal vector  $\vec{n}$  (see Fig. 3a). The second primary PEA-plane *P* is spanned using  $\vec{up}$  and  $\vec{n}$ . To enable the predictive animation, this plane is translated in  $\vec{dir}$  with positive offsets  $\gamma$ . An extension of this plane is the usage of multiple PEA-planes with different offsets  $\gamma$  (see Section 3.4).

**Complexity Reduction using Cutaway Surfaces.** Conventional rendering of 3D geometric models (see Fig. 1a) potentially hides relevant information or essential details due to perspective obstruction between these models. As we want to provide an unobstructed view of relevant anatomical structures while retaining contextual information, we employ cutaways. In our approach, the cutaway surface is defined as the visualization of a planar cross-section through an organ (the liver in this work), which can be interactively adapted by a tracked instrument (*in-plane*). This technique aims to overcome the

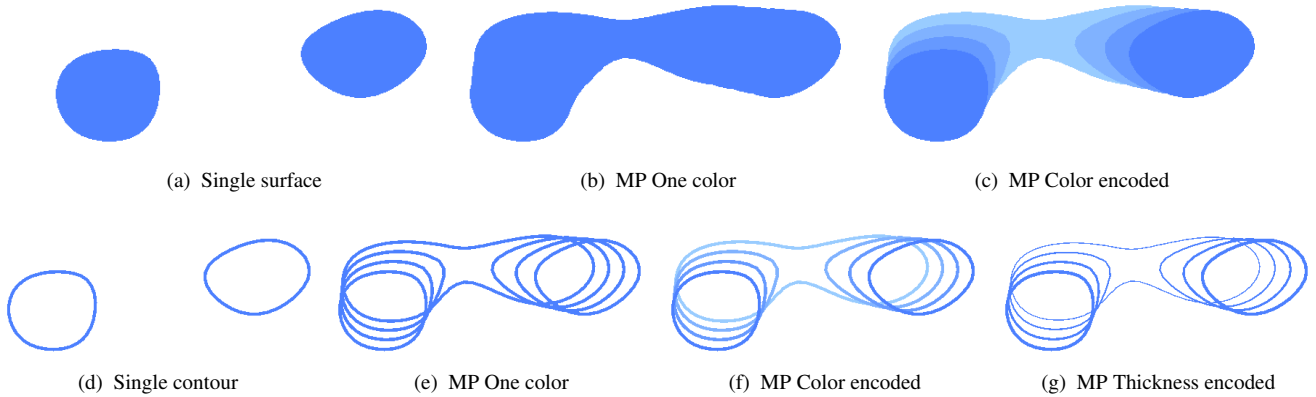


**Figure 4:** The images show different parameterization. Top row: cutaway surfaces with color encoding. Bottom row: contour lines with color and thickness encoding. Single plane and multiple planes (MP).

occlusion problem and reduces the visualization to a single plane, which shows all surfaces that intersect the defined planes  $CU$  or  $P$  and includes the 3D geometric models of all anatomical structures of the liver, vasculature and lesions.

The cutaway surface is implemented using a texture-based approach with OpenGL Framebuffer Objects (FBO). For each 3D geometric model, a single framebuffer texture is generated that contains all cut surfaces of the intersections between an implicit equation of a plane ( $Ax + By + Cz + D = 0$ ) and, e.g., the portal vein or tumor. These FBOs are then combined into a final cutaway surface texture that contains the information of the all intersections. Besides this final texture, this algorithm allows the combination of individual FBOs to visualize only specific structures (e.g., only the portal vein; defined as uniform shader parameter). This reduces the complexity to a specific structure and simplifies the visualization even more.

**Preservation using Contours Lines.** We use contour lines to enhance the cutaway surface with additional non-visible information about structures at risk (e.g., vasculature) in adjacent layers to the surface (*out-of-plane*). Therefore, we define the contour lines as an intersection of the planes  $CO$  with an offset  $\pm\delta$  (anterior and posterior) to  $CU$  or posterior to  $P$  and the 3D anatomical models (see Fig. 3a). Thus, the contours are defined as the loci of points  $\mathbf{p}$  for which  $\langle \vec{n}, \mathbf{p} \rangle = \delta$  holds, where  $\vec{n}$  denotes the plane normal and  $\delta$  the offset. The offset  $\delta$  acts as a safety margin and is defined by a predefined risk distance or distance between the preoperatively acquired radiological images (slice thickness or voxel size), in which structures should be visible to prevent complications. The depth, or rather distance between cutaway surface and contour planes, can be visualized with two visual encodings, motivated by Everts et al. [EBRI09]. Firstly, the larger the distance between the planes and the observer, the thinner the contour becomes and, secondly, the color brightness is modulated by the distance, with higher distances leading to lighter colors (distance encoding).

The contour lines are generated by a GLSL geometry shader with distance dependent contour thickness and color as described above.

Accordingly, the intersections between a plane and the triangles of the geometry are calculated. Therefore, for every vertex  $\mathbf{p}_i$ ,  $i \in \{1, 2, 3\}$  on a triangle of a 3D anatomical model, the value  $\varphi_i = \langle \vec{n}, \mathbf{p}_i \rangle - \delta$  is determined. If the sign of  $\varphi_i$  changes, a contour line is determined. Therefore, two points on two edges of this triangle will be connected. Suppose the following conditions hold:  $\varphi_1 > 0$ ,  $\varphi_2 > 0$  and  $\varphi_3 < 0$ . Then, somewhere on the edge connecting  $\mathbf{p}_1$  and  $\mathbf{p}_3$  and on the edge connecting  $\mathbf{p}_2$  and  $\mathbf{p}_3$  is a contour. The values  $t_1 = (\varphi_1)/(\varphi_1 - \varphi_3)$  and  $t_2 = (\varphi_2)/(\varphi_2 - \varphi_3)$  are determined and multiplied with the edge connecting  $\mathbf{p}_1$  and  $\mathbf{p}_3$  and the edge connecting  $\mathbf{p}_2$  and  $\mathbf{p}_3$ , respectively. This yields the position of the contour on the edge. Afterwards, both points will be connected and new geometry is created for each intersecting mesh. Thereby, uniform shader parameter define the line thickness and desaturation.

### 3.4. Multiple Contours and Surfaces

Instead of a single plane, multiple planes  $P$  in front of the applicator's tip can be utilized with either the cutaway or contour rendering to provide a better overview and additional value. Therefore, we define planes  $P_i$ ,  $i \in \{1, 2, 3, \dots\}$  with different discrete offsets  $\gamma_i \in \{1\text{ mm}, 2\text{ mm}, 3\text{ mm}, \dots\}$ . This offset and the number of planes are used by the shader to translate the cutaway plane accordingly. Thus, it is possible to determine the spatial relationships of the anatomical structures better and derive the course and distance on and around the path. Since the distances between the applicator's tip and the planes in front are defined by a fixed value, the correct depth can be derived. This represents additional information about possibly critical areas. Fig. 4 shows this approach with different parametrizations of both techniques. On the one hand, we used multiple color encoded cutaway surfaces. On the other hand, multiple contour lines are encoded using color and line thickness.

Figure 5 demonstrates examples of multiple contours and surfaces, each having specific advantages. The first case concerns blood vessels of different diameters that cross each other. With conventional rendering, the vessel that is farther away would be obstructed by the vessel closer to the viewer. This is a dangerous situation, since the

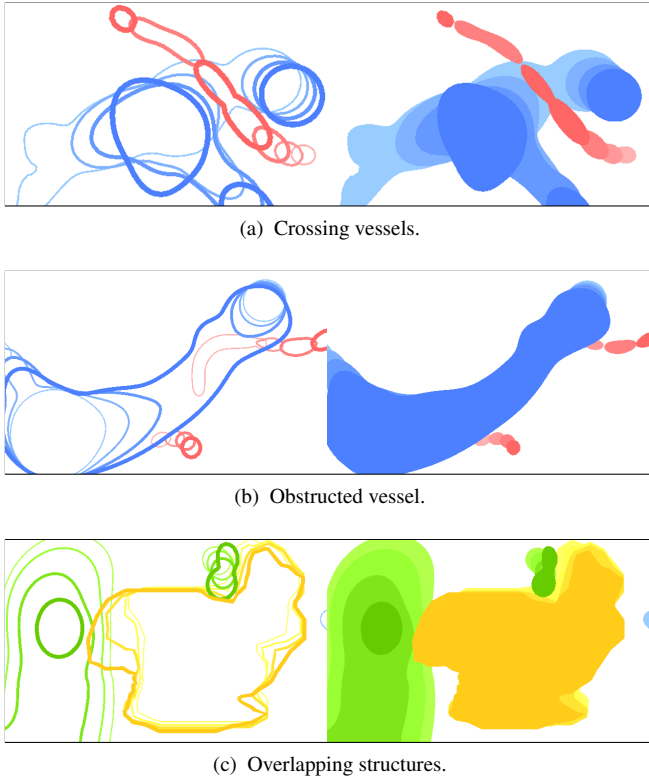


**Figure 5:** The images show different cases for multiple contours (left) and surfaces (right). (a) Completely crossing structures can be distinguished with both visualizations. (b) The path of hidden structures is not detectable using surfaces. (c) Overlapping structures and distances can be identified with contours but not with surfaces.

connectivity of the former vessel might be wrongly perceived. With our proposed approach, this problem is tackled and their spatial relationship visually well-perceivable. Using the surface visualization, the connectivity of these structures is better visually conveyed. The second case concerns partially or fully obstructed blood vessels. This is a dangerous situation, since the course of the obstructed vessels remains unknown. Using the contour visualization of our approach, this becomes clearly visible. These contours become smaller and lighter with increasing distance from the viewer. The third case deals with partially overlapping 3D anatomical structures. Again, with conventional rendering methods, the course of the structure or the distance to the other structures cannot be recognized in the overlapping regions. Using our contour-based approach, this is visually conveyed and well-perceivable.

### 3.5. Predictive Echo Animation (PEA)

Echo sounding or echolocation uses sound pulses to determine the distance of objects for their localization within an environment. We used this principle to visualize the course of anatomical structures on a planned applicator path. Besides being applied to a planned path, this technique can be utilized on any path that is defined by a position and orientation of a tracked instrument. This method is a tool that

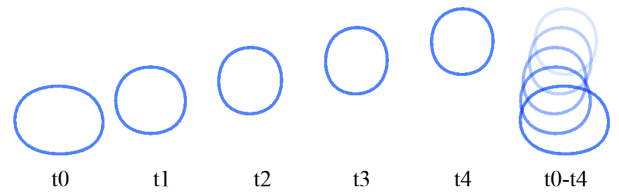


**Figure 6:** Different time steps  $t_i$  of the predictive echo animation. The right image shows the combination of several time steps, depicting the course of an anatomical structure.

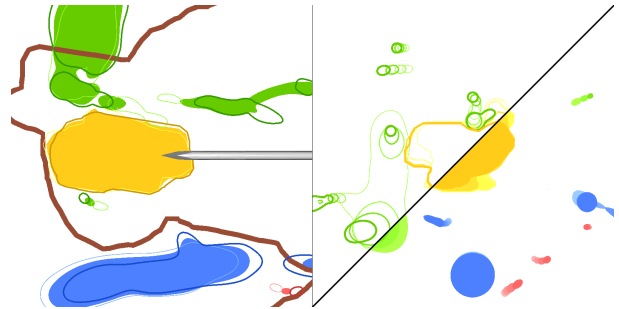


**Figure 7:** Linked View with an applicator approaching a tumor. Left (V1) shows the structures that are in-plane as surfaces and out-of-plane as contours. Right (V2) shows a split screen of multiple contours and surfaces.

allows surgeons to determine the depth or rather distance between the applicator’s tip and structure in front of it. Furthermore, course, shape and spatial relationships of the vasculature can be derived. In this way, a prediction of upcoming areas at risk is possible.

To implement this technique, the plane (or planes)  $P$  is translated over time along  $\vec{dir}$ , or the planned path, and is intersected with each geometry on its trajectory (see Fig. 6). This results in a simulation or rather a virtual slicing through the 3D anatomical model, similarly to the conventional and familiar slicing through radiological images. Accordingly, all anatomical structures between the applicator’s tip and a target on the path can be assessed in a short period of time.

### 3.6. Linked View

The linked view (see Fig. 7) is the combination of the map displays for the planes  $CU$  with its adjacent planes  $CO$  (V1) and  $P$  (V2). Thereby, arbitrary variations of cutaway surfaces and contours lines can be combined in one view. Display V1 presents all anatomical structures (in- and out-of-plane) in the applicator’s direction as a cutaway surface, if the structure is on the plane, and as color and thickness encoded contour in the adjacent planes. Display V2 shows the anatomical structures on the applicator path across. This linked view facilitates surgeons with a comprehensive overview of all critical and delicate anatomical structures along as well across the applicator path.

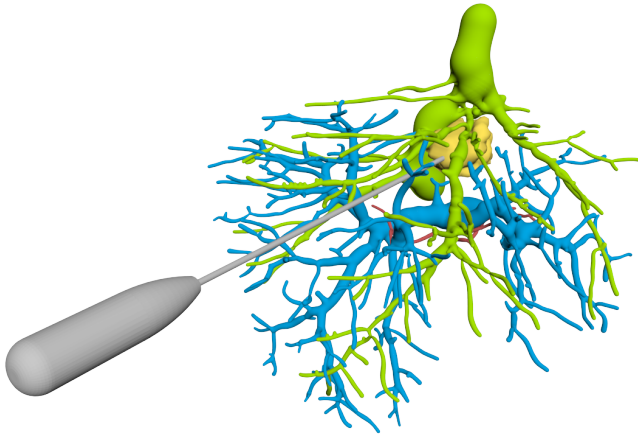


**Figure 8:** Example of a surface rendering of a 3d anatomical liver dataset with colored vasculature and an ablation applicator.

#### 4. Evaluation

To provide feedback, we evaluated our approach within two studies. Firstly, we performed a quantitative pilot study consisting of only static images created by our approach, evaluating the task completion time and error rate. Secondly, a interactive user study was conducted with several domain experts, to assess the visual encoding of the color and line thickness as well as the value of the PEA. Both studies are subsequently described.

##### 4.1. Quantitative Pilot Study

This pilot study aims to answer the question in which way the user’s assessment of structures at risk differs between a conventional clinical 3D visualization and our map display. The study was performed under controlled lab conditions, to achieve a steady and repeatable setup. We used three different liver data sets with 3D anatomical models of the portal vein (blue), hepatic vein (green), hepatic artery (magenta), and tumor (yellow) (see Fig. 8). For each of the three data sets, five applicator paths were defined with different orientations and distances to structures of high risk ( $N = 15$  applicator positions for each visualization).

At the beginning, each participant was given a short introduction on the study purpose. Then, we showed an exemplar visualization to explain how the different 3D anatomical models can be identified and how the map display is interpreted. Furthermore, participants were asked to practice interaction with the 3D visualization for as long as they desired. Afterwards, we presented a sequence of five stimuli (applicator paths) for each data set. These stimuli were presented in a randomized order on a monitor and consisted of a conventional clinical 3D visualization (standard shaded 3D surface rendering) and our map display. Each participant had to subsequently answer the following two questions:

1. Is the instrument tip in close proximity to critical structures ( $<1$  cm)?
2. If answered with yes: To which structure? The hepatic vein, portal vein, hepatic artery, or tumor.

**Table 1:** Results of the risk structure assessment around the applicator tip (summed over all participants) as well as mean value and standard deviation of task completion time (in seconds) for our map display and the conventional 3D surface rendering.

Visualization	$\Sigma$ fp	$\Sigma$ fn	Time [s]
Map Display	25	24	$11.82 \pm 04.48$
3D Standard	30	38	$40.49 \pm 36.38$

For each applicator position, we measured the time to identify the critical structures and recorded the given answers. A total of 60 assessments had to be made for both visualizations (conventional 3D and map display). For distance estimation, a printout with hints was provided, including the applicator diameter, the tip size, and the size of the risk radius (safety margin) around the applicator’s tip. Furthermore, the distance (5 mm) between the planes was known by the participants. No additional hints (e.g., distance or risk analyses) were displayed in either visualization, so as to solely identify the benefit of the map display. During the experiments, we followed the think-aloud protocol [FKG93] to gather individual and qualitative information about problems and improvements.

##### 4.2. Interactive User Study

The interactive user study with domain experts was performed informally, i.e., no specific task had to be fulfilled, to assess the advantages and disadvantages of our map display and the PEA. As before, the study was performed under controlled lab conditions. For the evaluation of the color and thickness encoding of the two methods, we presented a series of four cases with ten different parameter sets ( $N = 40$ ). Figure 9 presents some images of our user study including different overlapping anatomical structures. To evaluate the PEA, we used four different visualizations and showed videos of an applicator that was inserted into a liver targeting a tumor.

#### 5. Results

The **quantitative pilot** study comprised eleven participants (average age = 32 years, 3 female and 8 male) with different levels of experience in medical visualization (mean = 3.45 based on a 5-point Likert scale from 1 = none to 5 = much). Six participants were computer scientists and experts in visualization as well as computer-assisted surgery, and five were scientists of an anatomical institute. The results regarding task completion time (assessment time), False Positive (fp) and False Negative (fn) rated structures are shown in Table 1. The collected data were analyzed with a Wilcoxon signed-rank test for dependent samples. The analysis provides the following results (see Table 2). The comparison of the error rates of our map display and 3D visualization results in, with  $z = 2.06$  ( $p = .002 < .05$ ), significantly fewer false assessments (fp + fn) favoring our approach. Also, with  $z = 2.94$  ( $p < .001 < .05$ ), map displays enable significantly faster assessments.

In the **interactive user study**, six domain experts (average age = 29.5 years, 2 female and 4 male) with an average of 3.0 years of medical experience as physician were examined. For the informal

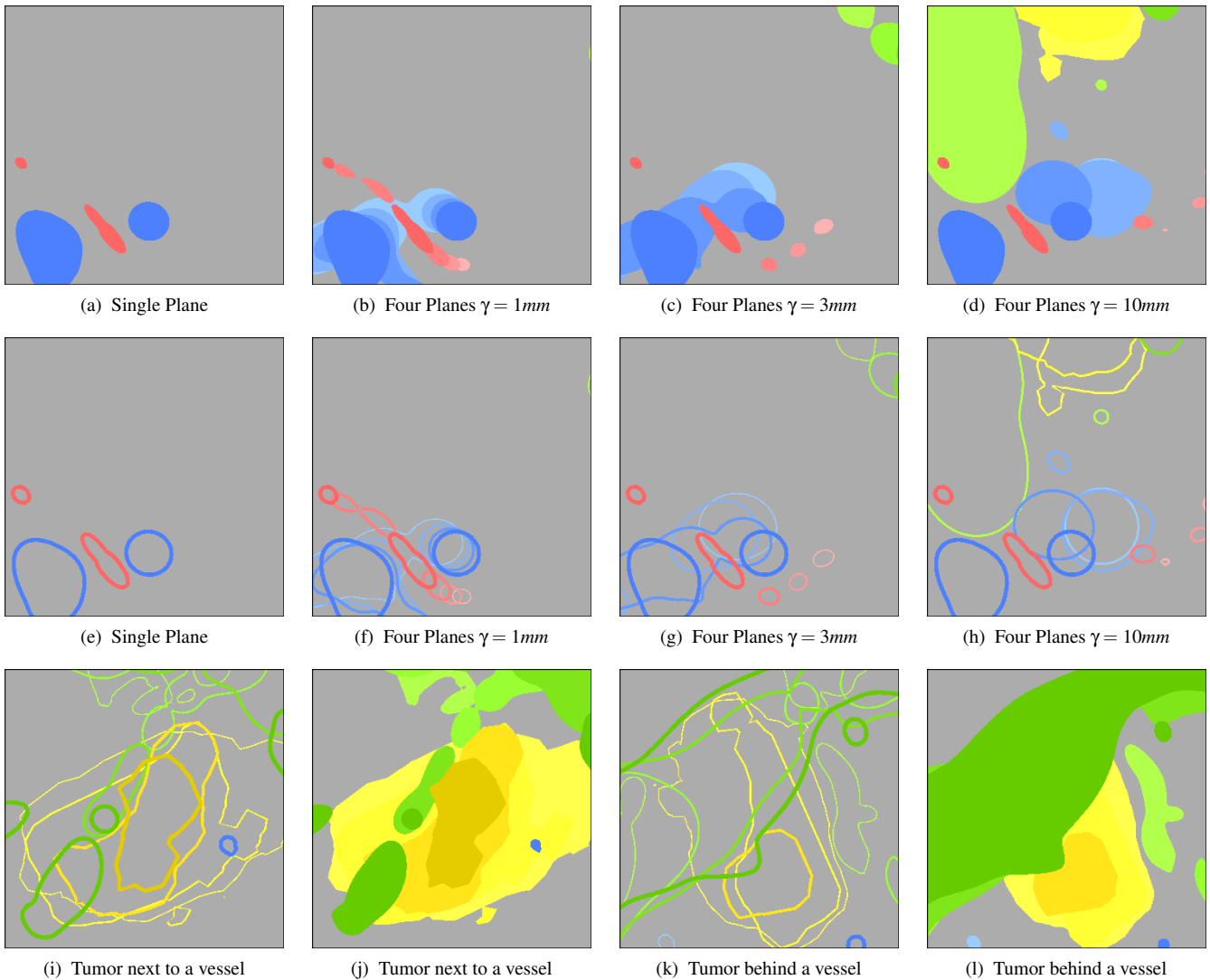


**Figure 9:** This figure showcases exemplary cases of two data sets used in the interactive user study. Top row: surface plane renderings with different plane offsets. Middle row: contour renderings with different offsets. Bottom row: two cases with overlapping structures.

evaluation, we used a simple questionnaire to assess different features of the visualization and the benefits and drawbacks of the PEA. Additionally, a statement for each question was retrieved. All results are presented in Fig. 10. The majority of the participants preferred the simple cutaway visualization with multiple slices (see Fig. 4c) for a still image (4 of 6). This is justified by the fact that radiological images show the surface of a structure as well and the contours would be mentally filled to resemble a surface. The multiple slices provide a better overview, since the participants were able to infer spatial relationships and course of vessels (5 of 6). The color and line thickness encoding were preferred compared to no encoding, because the human visual perception of depth and distances is based on the same principle (6 of 6). A combination of both to encode the depth was stated to be the most intuitive and could also be used by color-blind users.

In contrast to the evaluation of the individual encodings, where the cutaway surface was superior, both techniques are equal for the PEA (3 of 6). Using the animation, all participants were able to infer the shape, course and spatial relationships of the 3D anatomical structures with both visualizations. However, the contours were rated to allow a better visual depiction of partially obstructed structures, leading to a more precise assessment.

Overall, the evaluation confirmed the potential of the PEA to support the depiction of 3D anatomical structures in front of the applicator. It also allows surgeons to quickly spot critical structures on the applicator path. Nevertheless, the PEA visualization could be improved in several aspects, which is discussed in the following section in detail.

**Table 2:** Statistical Wilcoxon analysis of the assessment of critical structure and the task completion time (z: normalized T-value and p: probability of differences while expecting null hypothesis with  $\alpha = 0.05$ ).

Wilcoxon	z-value	p-value
False Positive (fp)	0.96	0.22
False Negative (fn)	1.78	0.051
Task Completion Time	2.94	< 0.001
fp + fn	2.06	0.002

## 6. Limitations and Discussion

According to the feedback gathered by the think-aloud protocol, our map display allows the anticipation of 3D anatomical structures that might be obstructed in other visualizations. We intentionally did not show any additional visual hints like analyses of different areas, e.g., distance between tumor and vasculature or the blood supply of the vessels, as proposed by Hansen et al. [HZR\*13]. Furthermore, no distances to the applicator’s tip were visually encoded. With this setup, we avoided any potential influencing factors and focused on the evaluation of our approach in comparison to a conventional 3D visualization. Based on the underlying 3D geometry, the integration of additional information such as distances or analyses would be possible and could provide an even better assessment of areas at risk.

Instead of a simple projection of the whole path, we only show a fixed area around and in front of the tracked applicator. This limits our approach, since an observer does not see directly if the path between applicator tip and target is free of obstacles. However, we were able to show that it is possible to get a better understanding of the depth of structures in front of the applicator. Moreover, the PEA provides an animation that shows the entire path in a short period of time; accordingly, all necessary information can be identified.

Compared to an MPR that is controlled by the applicator, our results show that it is easier to distinguish structures and infer spatial relationships without additional interaction. Since our visualization is based on the placement of a navigated applicator, the registration might influence the accuracy of our approach. Furthermore, motion and deformation of the organ is not incorporated, but this applies to an MPR as well. If a physically based algorithm, as presented by Peterlík et al. [PDC12], could transform the 3D anatomical structures with interactive frame rates (30Hz) it would be possible to incorporate this transformation and visualize the deformation on our map display, too.

All proposed algorithms are implemented using the OpenGL shader pipeline. This enables interactive frame rates (>30 Hz) and, accordingly, the direct interaction with a tracked instrument. The visual quality is in direct relation with the resolution of the generated 3D geometry and does influence the performance directly, i.e., a high screen and model resolution would decrease the frame rate and consequently would affect the interactivity.

Based on the feedback gathered during the evaluation, the animation style could be improved. A single translation might give a first

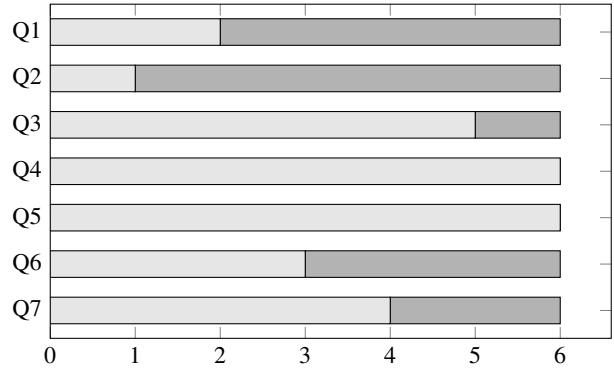


**Figure 10:** Results of the interactive user study. The diagram shows the answers of our six domain experts for the following questions. The questions Q1 to Q4 asked about the participants preference concerning the visual appearance. (Q1: contour/surface, Q2: one slice/multiple slices, Q3: dark to bright/bright to dark color encoding and Q4: thick to thin/thin to thick line encoding). Questions Q5 to Q7 assessed the benefits of the animation. (Q5: better overview between animation/image, Q6: higher accuracy between animation/image and Q7: which visualization method contour/surface)

overview, but some important structures could be missed. Accordingly, more than one *echo pulse* or other pattern, e.g., back and forth in a defined interval like well-known interaction with radiological images, should be considered. Furthermore, the control of the animation using the surgeons input could improve the perception even more, as a direct link between visualization and interaction exists.

## 7. Conclusions and Future Work

In this work, we propose an interactive map display for navigated applicator placement for liver interventions. Our approach combines cutaway surfaces and illustrative rendering techniques. While the cutaway surface visualizes structures that are in-plane to a defined applicator trajectory, contour lines provide contextual information to each anatomical structure. Additionally, both techniques can be applied to visualize structures in front of the applicator. An extension of this view uses animation to provide a virtual echo sound to identify anatomical structures between the current applicator position and a target structure with a single and multiple planes. The position and orientation of the map display is interactively controlled by a tracked applicator, which is actively used by the surgeon performing the intervention. Consequently, no cumbersome or time-consuming direct interaction with the navigation system is required. We showed that a simple cutaway visualization of 3D anatomical structures with additional context information in terms of contour lines has certain benefits. The results of our conducted user study confirm that our map display achieved a significantly better judgment of distances. Furthermore, the task completion time is less, due to the missing necessity of interaction and the easier visual representation. The statistical analysis for the task completion time was significant ( $p < 0.001$ ), favoring our map display. These results provide a foundation for further investigation and extensions to improve our visualization concept.

In conclusion, the evaluation demonstrated the benefits of the proposed map display and the advantages of the animation to assess structures at risk more efficiently and is less error prone. Despite the advantages of to contour rendering, future work could improve the visualization concerning overlapping structures with an adaptive algorithm combining contours and surfaces. Furthermore, the value of incorporated risk analyses and explicit regions of interest should be investigated. Additionally, a more detailed comparison between different cutaway visualizations, e.g., using volume data, would be interesting. Finally, a merged visualization of radiological images and our map display could be considered.

## Acknowledgment

This work is partially funded by the Federal Ministry of Education and Research (BMBF) within the STIMULATE research campus (grant number 13GW0095A) and the German Research Foundation (grant number HA 7819/1-1 and LA 3855/1-1).

## References

- [BBBV12] BIRKELAND Å., BRUCKNER S., BRAMBILLA A., VIOLA I.: Illustrative membrane clipping. *Computer Graphics Forum* 31, 3 (June 2012), 905–914. presented at EuroVis 2012. 4
- [BBW\*14] BANZ V. M., BAECHTOLD M., WEBER S., PETERHANS M., INDERBITZIN D., CANDINAS D.: Computer planned, image-guided combined resection and ablation for bilobar colorectal liver metastases. *World journal of gastroenterology: WJG* 20, 40 (2014), 14992. 2
- [BF08] BURNS M., FINKELSTEIN A.: Adaptive cutaways for comprehensible rendering of polygonal scenes. *ACM Trans. Graph.* 27, 5 (2008), 154:1–154:7. 4
- [BGKG05] BRUCKNER S., GRIMM S., KANITSAR A., GRÖLLER M. E.: Illustrative context-preserving volume rendering. In *Proceedings of the Seventh Joint Eurographics / IEEE VGTC Conference on Visualization* (2005), EUROVIS'05, pp. 69–76. 4
- [BMT\*16] BANZ V. M., MÜLLER P. C., TINGUELY P., INDERBITZIN D., RIBES D., PETERHANS M., CANDINAS D., WEBER S.: Intraoperative image-guided navigation system: development and applicability in 65 patients undergoing liver surgery. *Langenbeck's Archives of Surgery* 401, 4 (2016), 495–502. 2
- [DMNV12] DÍAZ J., MONCLÚS E., NAVAZO I., VÁZQUEZ P.: Adaptive cross-sections of anatomical models. *Comput. Graph. Forum* 31, 7pt2 (Sept. 2012), 2155–2164. 4
- [EBRI09] EVERTS M. H., BEKKER H., ROERDINK J. B., ISENBERG T.: Depth-dependent halos: Illustrative rendering of dense line data. *IEEE Transactions on Visualization and Computer Graphics* 15, 6 (2009), 1299–1306. 6
- [FKG93] FONTEYN M. E., KUIPERS B., GROBE S. J.: A description of think aloud method and protocol analysis. *Qualitative Health Research* 3, 4 (1993), 430–441. 8
- [HMP\*12] HERGHELEGIU P., MANTA V., PERIN R., BRUCKNER S., GRÖLLER M. E.: Biopsy planner - visual analysis for needle pathway planning in deep seated brain tumor biopsy. *Computer Graphics Forum* 31, 3 (June 2012), 1085–1094. 3
- [HWR\*10] HANSEN C., WIEFERICH J., RITTER F., RIEDER C., PEITGEN H.-O.: Illustrative Visualization of 3D Planning Models for Augmented Reality in Liver Surgery. *Int J Comput Assist Radiol Surg* 5, 2 (2010), 133–141. 4
- [HZR\*13] HANSEN C., ZIDOWITZ S., RITTER F., LANGE C., OLDHAFAER K., HAHN H. K.: Risk maps for liver surgery. *International Journal of Computer Assisted Radiology and Surgery* 8, 3 (May 2013), 419–428. 3, 10
- [HZS\*10] HANSEN C., ZIDOWITZ S., SCHENK A., OLDHAFAER K., LANG H., PEITGEN H.-O.: Risk maps for navigation in liver surgery. In *Proc. of SPIE Medical Imaging* (2010), vol. 7625, pp. 762528–1–8. 3
- [LCKM05] LIANG R. H., CLAPWORTHY G. J., KROKOS M., MAYORAL R.: Real-time predefined shape cutaway with parametric boundaries. In *International Conference on Computer Graphics, Imaging and Visualization (CGIV'05)* (2005), pp. 227–231. 4
- [LJPLD08] LAMATA P., JALOTE-PARMAR A., LAMATA F., DECLERCK J.: The resection map, a proposal for intraoperative hepatectomy guidance. *International Journal of Computer Assisted Radiology and Surgery* 3, 3 (2008), 299–306. 3
- [LLPH15] LAWONN K., LUZ M., PREIM B., HANSEN C.: Illustrative Visualization of Vascular Models for Static 2D Representations. In *International Conference on Medical Image Computing and Computer Assisted Intervention (MICCAI)* (2015), pp. 399–406. 4
- [LLS\*10] LAMATA P., LAMATA F., SOJAR V., MAKOWSKI P., MAS-SOPTIER L., CASCIARO S., ALI W., STÜDELI T., DECLERCK J., ELLE O. J., EDWIN B.: Use of the resection map system as guidance during hepatectomy. *Surgical Endoscopy* 24, 9 (2010). 3
- [LP16] LAWONN K., PREIM B.: *Feature Lines for Illustrating Medical Surface Models: Mathematical Background and Survey*. Springer Verlag, 2016, ch. Visualization in Medicine in Life Sciences III, pp. 93–132. 4
- [NC\*89] NETTER F. H., COLACINO S., ET AL.: *Atlas of human anatomy*, vol. 11. Ciba-Geigy Summit, NJ, 1989. 4
- [NGB\*09] NEUGEBAUER M., GASTEIGER R., BEUING O., DIEHL V., SKALEJ M., PREIM B.: Map Displays for the Analysis of Scalar Data on Cerebral Aneurysm Surfaces. In *Computer Graphics Forum (EuroVis)* (2009), vol. 28 (3), pp. 895–902. 4
- [NTS\*10] NAVKAR N. V., TSEKOS N. V., STAFFORD J. R., WEINBERG J. S., DENG Z.: Visualization and planning of neurosurgical interventions with straight access. In *Proc. of the First International Conference on Information Processing in Computer-Assisted Interventions* (2010), pp. 1–11. 3
- [PDC12] PETERLÍK I., DURIEZ C., COTIN S.: Modeling and real-time simulation of a vascularized liver tissue. In *Proceedings of the 15th International Conference on Medical Image Computing and Computer-Assisted Intervention - Volume Part I* (2012), MICCAI'12, pp. 50–57. 10
- [RBH\*11] RITTER F., BOSKAMP T., HOMEYER A., LAUE H., SCHWIER M., LINK F., PEITGEN H. O.: Medical image analysis. *IEEE Pulse* 2, 6 (2011), 60–70. 5
- [RWS\*10] RIEDER C., WEIHUSEN A., SCHUMANN C., ZIDOWITZ S., PEITGEN H.-O.: Visual support for interactive post-interventional assessment of radiofrequency ablation therapy. In *Proceedings of the 12th Eurographics / IEEE - VGTC Conference on Visualization* (2010), EuroVis'10, pp. 1093–1102. 4
- [SCC\*04] STRAKA M., CERVENANSKY M., CRUZ A. L., KOCHL A., SRAMEK M., GROLLER E., FLEISCHMANN D.: The vesselglyph: focus context visualization in ct-angiography. In *IEEE Visualization 2004* (Oct 2004), pp. 385–392. 3
- [SHP11] SCHENK A., HAEMMERICH D., PREUSSER T.: Planning of image-guided interventions in the liver. *IEEE Pulse* 2, 5 (2011), 48–55. 3
- [SPY\*15] STÄTTNER S., PRIMAVESI F., YIP V. S., JONES R. P., ÖFNER D., MALIK H. Z., FENWICK S. W., POSTON G. J.: Evolution of surgical microwave ablation for the treatment of colorectal cancer liver metastasis: review of the literature and a single centre experience. *Surgery Today* 45, 4 (2015), 407–415. 2
- [VKG04] VIOLA I., KANITSAR A., GRÖLLER M. E.: Importance-driven volume rendering. In *Visualization IEEE* (2004), pp. 139–145. 3, 4